Free form surfaces

J. Cotrina Navau, N. Pla Garcia

Departament de Llenguatges i Sistemes Informàtics, Universitat Politècnica de Catalunya, Av. Diagonal 647, 8ª, 08028 Barcelona.

e-mail: jcotrina@lsi.upc.es

Abstract

A method to construct C^k continuous surfaces of arbitrary topological type by tracing a mesh that represents a 2-manifold is presented. The presented approach constructs the surface from a collection of pieces which overlap, using the known technology of manifolds. The surface is built from the given mesh and two arbitrary input parameters, k and n. The value of k gives the continuity of the resulting surface and n controls the local influence of the vertices of the mesh.

The presented scheme generalizes the B-spline approach in terms of manifolds. The surface that arises from regular zones of the mesh is a tensorial product B-spline surface. For the rest, that is, the irregular zones, the surface has the following good properties: it is C^k continuous, affine invariant, the convex hull property is guaranteed, and it has local control. The algorithm is simple and efficient in time and space.

Key words: C^k-surfaces, manifolds, splines.

1 Introduction

The B-spline scheme, for simplicity and the properties of the resulting surfaces, is one of the methods more used in the representation and generation of surfaces in the computer aided geometric design (CAGD).

Even thought, the B-spline scheme is limited to regular control meshes. That is, each interior point of B-splines meshes must be regular, surrounded by exactly four quadrilateral mesh cells. This request only allows to represent objects that are deformations of the plane or the torus. Very simple objects, like a cube, can't be represented.

This problem has been one of the central problems in the CAGD. Several approaches have been proposed to obtain arbitrary topological surface models, but no satisfactory solution has been given, and no one that generalizes the B-spline scheme. Most of the existing methods are able to generate surfaces with continuities of order 1, and at most 2, or they are very expensive in time and/or space.

Algorithms based on recursive subdivision of the mesh are proposed in [CC 78], [D 78], [SZSS 98] and [Stam 98]. These algorithms yield a smooth surface with continuity order at most 2, and have been popular because of their simplicity and intuitive corner cutting interpretation.

Another approach is to refine the irregular input mesh, isolating regions of irregular points, and to fill in the irregular parts with a collection of triangular or rectangular Bézier patches (see [Wi 86], [HoMo 90], [Lo 94], [GZ 94], [Pe 95], [Reif 95]). The main drawback of these methods is that the resulting surface is GC^1 or GC^2, or the surface results from a local and usually expensive process.

A similar technique is to define n-sided patches to fill in the non rectangular parts of the mesh (see [LD 89] and [LD 90]). These approaches, as B-patches [Sei 91], provide elegant solutions, but the degree of the resulting surface is usually intractable.

Most of the mentioned methods solve the continuity constraint equations that arise from an irregular vertex or a n-sided hole, and this becomes more difficult as the continuity order increases. A similar approach is proposed in [Prau 97], but in this paper continuity constraint equations are proposed and solved in the parameter space (that is in $\mathbb{R}^2$), so it simplifies the process. The drawback of this method is the geometry of the resulting surface. Near an irregular vertex the surface always has constant curvature.

A different approach was proposed in [GH 95], based on the technology of manifolds. Grimm and Hughes propose to define the surface in two different parts: first, a manifold is built with the same topology as the original polyhedral mesh and second, geometry is added to the atlas defining control points. The solution is theoretically very interesting, but computationally expensive. The number of charts is very high and they are very small.

Following some of the ideas proposed in [GH 95], in [CP 99] we present a scheme for constructing C^k-surfaces from irregular control meshes that can be embedded in the plane. Although the method is not able to model arbitrary topological surfaces, because planar meshes only can model deformations of the plane, the fundamental ideas and the algorithm presented there, are now generalized here to work with arbitrary free form surfaces.

In this paper we present a method, based on the manifolds technology, that allows to model arbitrary topological objects, approximating control meshes not necessarily regulars, and obtaining surfaces of desired continuity order.

Where the mesh is regular, the obtained surface is a B-spline tensorial product surface. This property is important, for the quality of the surface and for the low cost, in time and space that this represents, because the irregularities are generally few. Moreover this ensures that B-spline scheme can be obtained as a particular case of the presented method.

Where the mesh is irregular, the proposed method ensures that the fundamental properties of B-spline scheme are satisfied, that is, affine invariance, convex hull property (global and local), a simple construction process, low degree surface and arbitrary geometric continuity order.

The input of our algorithm is a polyhedral mesh and two parameters n and k. The mesh describes the topology and the basic shape of the output surface, as in the B-spline case. The n value controls the influence of the control points and k is the continuity of the resulting surface.

This paper is organized as follows. Some preliminary definitions about graphs and manifolds are given in Section 2. An overview on the construction process is given in section 3. In section 4 a manifold with the same topology as the original mesh, and locally embedded in $\mathbb{R}^2$ is constructed. This manifold will be used as the parameter space to define the surface. In section 5 a basis function associated to each chart of the new manifold is defined and in section 6 the control points used to generate the surface are described. How to construct the surface is defined in section 7. In section 8 we discuss the implementation and a family of examples, and finally in section 9 the conclusions are exposed. In Appendix 11 are placed most of the technical results used in previous sections.

2 Background and Definitions

The approach presented in this paper begins with a polyhedral mesh that describes roughly the surface. This mesh can be understood as a graph or as a manifold, so some results of graph theory and manifold technology are necessary.

2.1 Graph theory

Most of the content of this section can be found in any book on graph theory (see for instance [Ma 71] or [Wh 73]).

A simple *graph* $G = G(V, E)$ is a non-empty set of vertices $V = \{v_i | i = 1, \ldots, m\}$ and a set of edges $E = \{\{v_i, v_j\}, \ldots, \{v_r, v_s\}\}$ where each edge $\{v_i, v_j\}$ is an unordered pair of different vertices. A vertex v_j is a *neighbor* of a vertex v_i if $\{v_i, v_j\} \in E$. The *degree* of a vertex v_i, d_i, is the number of edges incident to v_i, that is $d_i = |\{v_j \in V | \{v_i, v_j\} \in E\}|$.

A graph H is a *subgraph* of a graph G if both its vertices and edges belong to G.

A graph $G = G(V, E)$ can be embedded in a surface S if it can be draw on S, in such a way that edges only intersect at their common vertices, that means,

(1) each node $v_i \in V$ is mapped to a point in S,
(2) each edge $\{v_i, v_j\} \in E$ is mapped to a curve on S whose endpoints are the images of v_i and v_j,
(3) the only intersections between curves are at their common endpoints.

A graph G is said to be *planar* if it can be embedded in $\mathbb{R}^2$. A planar embedding of G is referred as a *plane graph.*

A plane graph partitions the plane into connected regions called faces. The unbounded face is called the *outer* face. The *boundary* ∂G of a graph G is the subgraph consisting of all vertices and edges witch are incident on the outer face.

Let H be a subgraph of a plane graph G, the $1 - face - layer$ of H, denoted by $fl_1(H, G)$, is defined as the graph determined by the union of H and the vertices and edges that belongs to the faces incidents to H, informally we are adding to H the layer of faces that surround it. In general we define $fl_i(H, G)$ as $fl_1(fl_{i-1}(H, G), G)$.

2.2 Manifolds

The technique that defines surfaces from pieces which overlap, that is, the manifold technology, is reviewed here. Manifolds have been studied for many years (see [Do 76] or [BG 88]). Manifolds are objects that locally behave like Euclidean spaces, thus, they can be studied in the same way.

A formal definition of manifold, taken from [GH 95], is given here. This definition is equivalent to the traditional one, [GH 95].

Definition 1 *A C^k differentiable proto-manifold K of dimension n consist of:*

(1) A finite collection A of connected open sets in $\mathbb{R}^n$. A is called a proto-atlas. Each element $c \in A$ is called a chart.
(2) A collection of open subsets $U_{i,j} \subset c_i$, for each c_i and c_j charts of A, with $U_{i,i} = c_i$.
(3) A set of transition functions Φ. A transition function $\phi_{i,j}$ is a map $\phi_{i,j} : U_{i,j} \longrightarrow U_{j,i}$ which is bijective and C^k-differentiable. These functions must hold:

$$(a)\ \phi_{i,j}^{-1} = \phi_{j,i}$$

$$(b)\ \phi_{i,i}(x) = x \quad \forall x \in c_i$$

$$(c)\ \phi_{j,k} \circ \phi_{i,j}(x) = \phi_{i,k}(x) \quad \forall x \in U_{i,k} \cap U_{i,j}$$

In the proto-manifold K, an equivalence relation is defined as follows:

$$\forall\, x \in c_i,\ \forall\, y \in c_j, \quad x \sim y \quad \textit{iff} \ \ \phi_{i,j}(x) = y$$

We can define $M = K/\sim$, the quotient of K by $\sim$, which is called a manifold.

3 Overview of the construction process

Let $G = G(V, E)$ be the initial control mesh, where $V = \{v_1, \ldots, v_r\}$ are the vertices (control points) of the mesh and E the edges that fixes the topology. Moreover, two parameters, $n > 1$ and $k > 0$, have also to be given. The value of n controls the local influence of each control point, and the parameter k is the continuity of the resulting surface.

To simplify the exposition, we are assuming that the original control mesh is a mesh without boundary, and the case of dealing with boundaries is placed in appendix 11.2. The construction process is divided in the following steps:

(1) First a two manifold M is built from the control mesh G, using the input parameters n and k. That is, a set of charts $\{C_i | i \in I\}$ and a collection of transition functions, $\{\phi_{ij}^k : C_i \to C_j | (i,j) \in I \times I\}$, which gives the overlaps between the charts. The resulting manifold M has the same topology of the original mesh G.
(2) For each chart, C_i, a non-negative basis function is defined: $\psi_i : \mathbb{R}^2 \to \mathbb{R}$ with support on C_i and with k-continuity. Each one of these functions, ψ_i, gives a non-negative function, N_i, defined on the manifold M with support on the image of the chart C_i. Thus, we have $N_i : M \to \mathbb{R}$. These functions are C^k and we assume that they form a partition of the unity on M, otherwise, they are normalized.
(3) A control point P_i is attached to each chart C_i, which gives the geometry of the resulting surface.

(4) Finally the surface is parameterized in M, using the basis functions $\{N_i^k | i \in I\}$ and the control points $\{P_i | i \in I\}$, following next expression:

$$x(u) = \sum_{i \in I} P_i N_i^k(u), \qquad u \in M$$

4 The manifold

In this section, a manifold is built with the same topology as the original control mesh. This manifold is used as the parameter space where the surface is defined.

The construction depends on the two input values n and k. Although the presented construction follows the same notions than in the planar case (see [CP 99]), this is the part of the algorithm which differs more from those case.

The construction is divided in different steps, which are detailed later on:

(1) A pre-process is applied to the original mesh which isolates the irregularities of the mesh and reduces the different types of irregularities.
(2) A collection of charts, that is, a collection of open subsets of $\mathbb{R}^2$, is defined from the refined mesh.
(3) Transition functions are built, which give the overlaps between the charts.
(4) Finally, a manifold with the same topology than the original mesh is obtained.

4.1 Pre-process

In order to simplify the construction, a pre-process is applied to the original mesh, based on the Catmull-Clark subdivision scheme [CC 78].

The aim of the pre-process is to obtain a mesh $G_1 = (V_1, E_1)$ defining roughly the same surface and with the following properties:

(1) All the faces of the mesh are four sided, thus all the irregularities are in the vertices.
(2) For any irregular vertex $v_i \in V_1$, the subgraph $fl_{n+1}(\{v_i\}, G_1)$ does not contain any other irregularity. That means that irregular vertices are sufficiently separated.
(3) For any vertex $v_i \in V_1$, the subgraph $fl_{n+1}(\{v_i\}, G_1)$ is a planar graph, that means, a graph that can be embedded in $\mathbb{R}^2$. Thus for any vertex there exists a sufficiently bigger planar neighborhood.

The Catmull-Clark subdivision process refines the given control mesh by adding new vertices following the rules:

(1) A new vertex is defined for any vertex, edge and face of the given control mesh.
(2) New edges are formed by connecting each new face point to the new edge vertex of the edge defining the old face.
(3) New edges are defined by connecting each new vertex point to the new edge points of all old edges incident on the old vertex.
(4) New faces are then defined as those enclosed by new edges.

The Catmull-Clark subdivision process has the following properties:

(1) The mesh can be of arbitrary topological type.
(2) After the first subdivision step all faces are quadrilaterals.
(3) The number of irregular vertices is fixed, and is equal to the number of irregular vertices in the mesh produced after the first subdivision, that is, the irregular vertices that corresponds to ones in the original mesh G and the new vertices corresponding to the non quadrilateral faces of the original mesh G.

These properties imply that given an arbitrary mesh G, after applying a finite number of Catmull-Clark subdivisions the resulting mesh G_1 fulfills the requests pointed before.

First, after one step of the Catmull-Clark subdivision, all the faces of the resulting mesh are quadrilaterals, thus the first condition is hold.

Second, given two arbitrary vertices v_i and v_j of the graph G, such that,

$$v_i \in fl_k(\{v_j\}, G) \setminus fl_{k-1}(\{v_j\}, G)$$

then, the vertices v_i' and v_j' corresponding to v_i and v_j respectively by a Catmull-Clark subdivision hold

$$v_i' \in fl_{2k}(\{v_j'\}, G') \setminus fl_{2k-1}(\{v_j'\}, G').$$

Indeed, in each step of the pre-process a layer of faces is divided in two different layers. Thus, the two previous conditions are obtained in the worse case, after $\log_2(n + \frac{1}{2}) + 2$ Catmull-Clark subdivisions.

4.2 The charts

Let us call $G = (V, E)$ the mesh obtained once the pre-process has been applied to the original mesh, where $V = \{v_1, \ldots, v_r\}$. The definition of the charts is

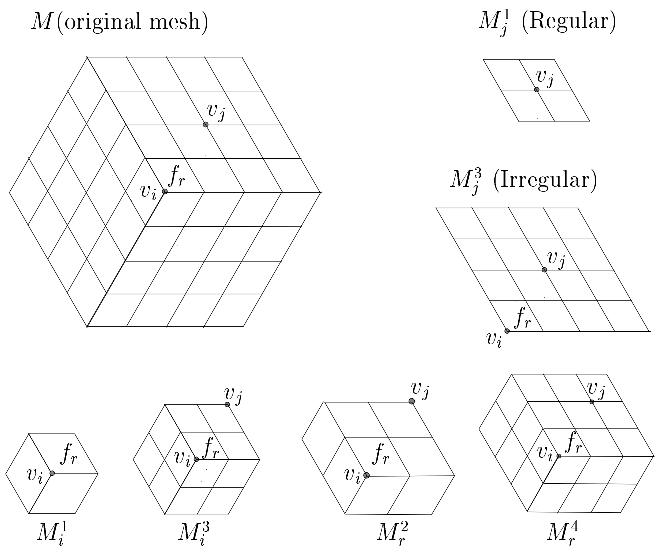

Figure 1. Subgraphs M_i^n.

divided, on its turn, in the following steps, which are detailed in the rest of the section:

(1) Subgraphs of G, M_i^n, are defined.
(2) The subgraphs M_i^n are embedded into $\mathbb{R}^2$, let R_i^n be its image.
(3) Charts $C_i^n \subset \mathbb{R}^2$ are defined using the subsets R_i^n.

Thus, first, subgraphs M_i^n of the mesh G, are considered. These subgraphs M_i^n are built using the following recursive definition:

(1) $M_i^{-1} = v_i$, for each vertex $v_i \in V$.
(2) $M_j^0 = f_j$, for each face f_j of G.
(3) In general, let $M_k^n = \bigcup_{M_k^{n-2} \subset M_j^{n-1}} M_j^{n-1}$ where $M_k^{n-2} \subset M_j^{n-1}$ means that M_k^{n-2} is a subgraph of M_j^{n-1}.

Using this definition, we can say that there exists a M_i^{-1} graph for every vertex of G and a M_j^0 graph for every face of the mesh. Moreover, when, n is an odd number, M_i^n is $fl_{(n+1)/2}(v_i, G)$, that is, is the subgraph of G defined by $(n+1)/2$-layers of faces around the vertex v_i. If n is an even number, then M_i^n is $fl_{n/2}(f_i, G)$, that is, is the subgraph of G defined $n/2$-layers of faces around the face by f_i (see figure 1).

The subgraphs M_i^n can be classified in two different groups, depending on the number of irregularities they have: *Regular subgraphs*, subgraphs with all the vertices regular, and *irregular subgraphs,* subgraphs with one irregular vertex.

The properties of the pre-process imply that the subgraphs M_i^n contain at most one irregularity and that they are planar graphs.

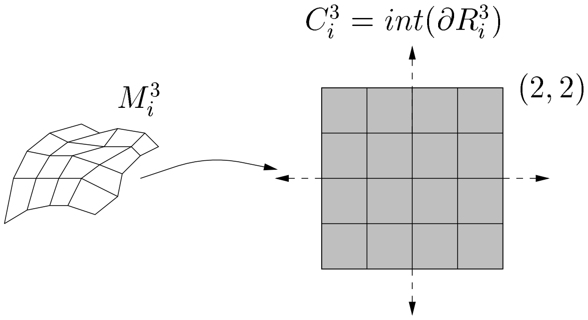

Figure 2. Regular chart, with $n = 3$.

Indeed, notice that when n is an odd number

$$M_i^n = fl_{\frac{n+1}{2}}(v_i, G) \subset fl_n(v_i, G)$$

for a vertex $v_i \in V$. Moreover, if n is an even number

$$M_i^n = fl_{\frac{n}{2}}(f_i, G) \subset fl_n(v_j, G)$$

where v_j is a vertex of the face f_i.

Thus, in both cases, M_i^n is a planar graph due to the property 3 of the pre-process.

Moreover, if $v_j \in M_i^n$ is a vertex, then

$$M_i^n \subset fl_{n+1}(v_j, G)$$

In particular, when M_i^n has an irregular vertex v_j, then

$$v_j \in M_i^n \subset fl_{n+1}(v_j, G)$$

Thus, M_i^n contains at most one irregular vertex (property 2 of the pre-process).

Any regular subgraph M_i^n is embedded into a regular mesh R_i^n, with sides parallel to the canonic axis, centered on the origin and with all the vertices uniformly placed (see figure 2).

Irregular subgraphs only contain one irregularity. For every irregular vertex v_l, we can define

$$Y_l^n = \cup_{v_l \in M_i^n} M_i^n$$

Using the properties of the pre-process, Y_l^n can be embedded into $\mathbb{R}^2$ and all the vertices are regular except v_l. Thus, Y_l^n is a irregular configuration which can be embedded into a regular star plane configuration X_l^{2n} (see figure 3). In appendix 11.1, the definition of the vertices of the X_l^{2n} star configuration is detailed. Therefore, for any irregular subgraph M_i^n, there exists an unique irregular configuration Y_l^n which includes it. And, the subgraph M_i^n is embedded in the corresponding regular star plane configuration X_l^{2n} in a natural

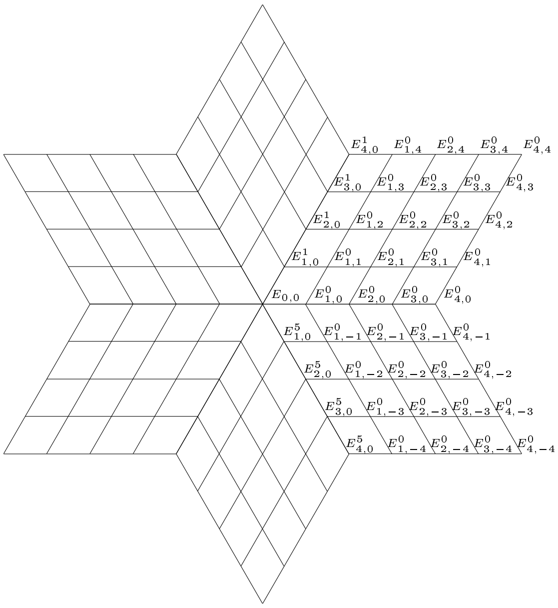

Figure 3. Regular star plane configuration with $g = 6$.

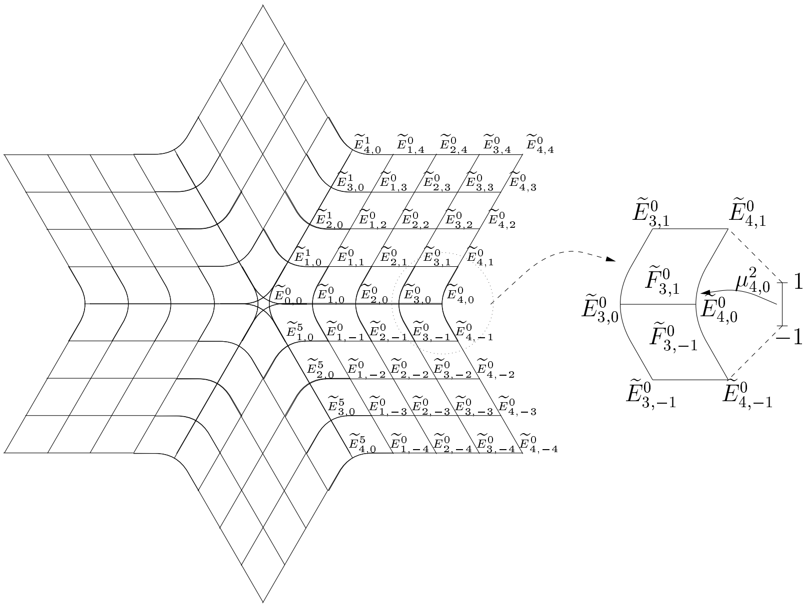

Figure 4. 2-continuous regular star plane configuration with $g = 6$

way. Let us call R_i^n the image of the subgraph M_i^n into $\mathbb{R}^2$ by the previous embedding.

In order to define the charts of the manifold, where continuous basis functions are built, a modification of the regular star plane configuration is used: the k-continuous regular star plane configuration: $\widetilde{X}_l^{2nk}$ (see figure 4).

As can be seen in appendix 11.1, the main properties of the k-continuous regular star configuration $\tilde{X}_l^{2nk}$ are that k-continuous curves join the vertices

E_{i1}^m and E_{i-1}^m and that the irregular vertex E_{00} blows up into $g = degree(v_l)$ different vertices $\tilde{E}_{00}^j$, where $j = 0, \ldots, g-1$.

Now, we are ready to define the charts of the manifold. There exists a chart C_i^n corresponding to any subgraph M_i^n.

If M_i^n is a regular subgraph, the interior set of R_i^n is taken as a chart, that is, $C_i^n = int(\partial R_i^n)$ which is an open set of $\mathbb{R}^2$. Using this definition, any interior vertex of M_i^n can be represented on the chart (figure 2).

In the irregular case, the construction depends on the parity of the n value. To simplify notations, let us give the following definitions:

$$
\begin{aligned}
\sigma(j) &= \begin{cases} 1 \text{ if } j \geq 0 \\ -1 \text{ if } j < 0 \end{cases} \\
\rho(n) &= (n+1) \bmod 2, \\
\xi(n,j) &= \frac{1}{2}\rho(n)\sigma(j), \\
w &= \frac{n+1}{2}.
\end{aligned}
\tag{1}
$$

Moreover, let us call $\tilde{F}_{i,j}^m$ the face determined by the vertices $\tilde{E}_{i,j-\sigma(j)}^m$, $\tilde{E}_{i,j}^m$, $\tilde{E}_{i+1,j-\sigma(j)}^m$, and $\tilde{E}_{i+1,j}^m$, see figure 4 for notation.

As has been pointed out, there exists a M_i^n subgraph for any vertex in the case of n odd and a subgraph for any face when n is even, thus to unify the construction in both cases, let us define:

$$
\tilde{e}_{i,j}^m = \begin{cases} \tilde{E}_{i,j}^m \text{ if } n \text{ is odd} \\ \tilde{F}_{i,j}^m \text{ if } n \text{ is even} \end{cases}
\tag{2}
$$

where $i = 0, \ldots, \lfloor w \rfloor$, $\mid j \mid = \rho(n), \ldots, i + \rho(n)$ and $m = 0, \ldots, g-1$. Then, a chart is attached to any element $\tilde{e}_{i,j}^m$. Let

$$
A = \tilde{E}_{i+w+\xi(n,i),j+w-\xi(n,j)}^m,
$$

$$
\begin{aligned}
B &= \tilde{E}_{i+w+\xi(n,i),j-w-\xi(n,j)}^m \\
\vec{v}_m &= \tilde{E}_{1,0}^m - \tilde{E}_{0,0}^m
\end{aligned}
$$

and the C^k curve C_{AB} from A to B, following the k-continuous regular star configuration (see 11.1). The set $R_{i,j}^m$ is defined as the result obtained from the drag of C_{AB} along the vector $-(n+1)\vec{v}_m$, placed in the point A. The chart $C_{i,j}^m$ is defined as the interior of $R_{i,j}^m$ (figure 5).

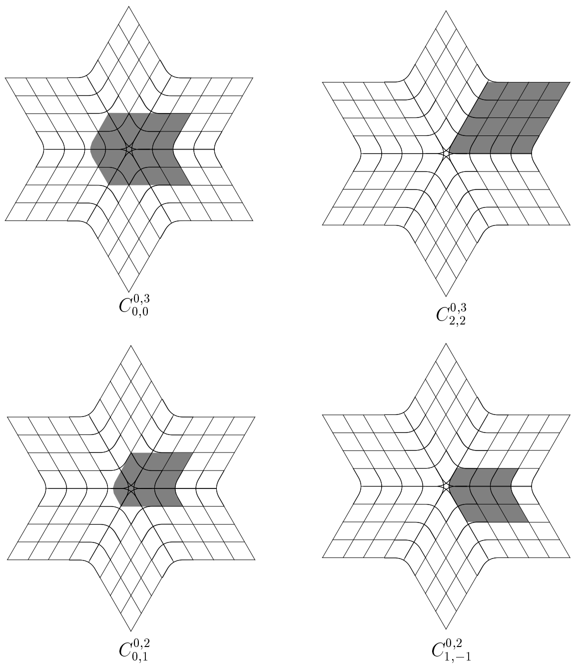

Figure 5. Irregular charts, with $n = 3$ and $n = 2$.

When n is odd, the irregular vertex blows up into g different vertices thus, there exist different elements $\tilde{e}_{00}^{m}$ for $m = 0, \ldots, g-1$ which are associated to the irregular vertex. In this case, the chart associated to the subgraph M_i^n corresponding to the irregular vertex is the union of the g charts defined from the elements $\tilde{e}_{00}^{m}$. The same is valid for the elements $\tilde{e}_{i,i}^{m} = \tilde{e}_{i,-i}^{m+1}$, which have a chart that is the union of two different sets (defined by the drag along $\vec{v}_m$ and $\vec{v}_{m+1}$).

4.3 The transition functions

Once a collection of charts have been defined, the next step is to define a set of transition functions that give the overlaps between these charts. These functions must be defined so that the resulting manifold, locally embedded in $\mathbb{R}^2$, has to be homeomorphic to the manifold that arises from the control mesh.

Different cases are distinguished in the definition of the transition functions, depending on the type of the involved charts:

Transition function between two regular charts: Let C_i^n and C_j^n be two regular charts. They are defined as the interior of a regular mesh with sides parallel to the canonic axis and with all the vertices uniformly placed. In this case the transition function $\phi_{i,j}^{k}$ is the identification of the faces of

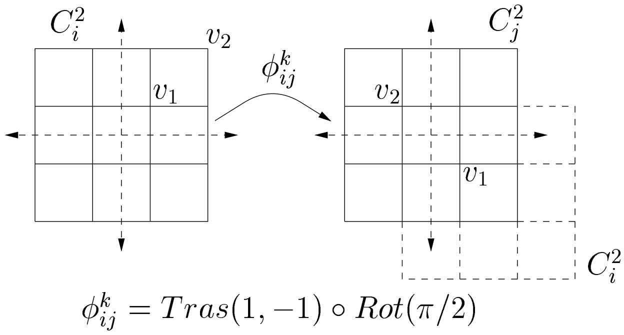

Figure 6. Transition function between regular charts.

the charts corresponding to the same face in the mesh G. The regularity and the uniformity of these charts imply that only rotations and translations are necessary. See figure 6.

Transition function between two irregular charts: Let C_i^n and C_j^n be two irregular charts. The transition function between these charts is not trivial, that means, the overlap between the charts is not empty only when they contain the same irregularity. In this case, both charts are included in the same $k-$*continuous* regular star configuration, and the transition function is defined as the identity map, between their intersection.

Transition function between a regular chart and an irregular chart: Let C_r^n be a regular chart and let C_s^n be an irregular chart. These two charts overlaps when they have faces corresponding to the same face of the graph G. In this case the regular chart $C_r^n = (-w,w)\times(-w,w)$ can be included in $\tilde{X}_l^{2nk}$ the regular k-continuous star configuration, that is, the vertices represented in C_r^n are also represented in $\tilde{X}_l^{2nk}$.

Let $\tilde{e}_{i,j}^m \in \tilde{X}_l^{2nk}$, with $\lfloor w \rfloor < i \leq n + \lfloor w \rfloor + 1$ and $\rho(n) \leq |j| \leq i + \rho(n)$, the element associated to M_r^n (and to the regular chart C_r^n). Using this notation we can consider (rotating C_r^n if necessary) that the vertex associated to $(w,w) \in \overline{C_r^n}$ is $\tilde{E}^m_{i+w+\frac{1}{2}\rho(n),j+w-\xi(n,j)}$.

Then, the embedding of C_r^n in $\tilde{X}_l^{2nk}$, $\hat{\phi}_{r,l}^k : C_r^n \to \mathbb{R}^2$, is defined as

$$\hat{\phi}_{r,l}^k(x,y) = \beta_{i,j,m}^k(y) + (x + \xi(n,i))\,\vec{v}_m, \tag{3}$$

where $\beta_{i,j,m}^k : (-w,w) \to \mathbb{R}^2$ is detailed in appendix 11.3.

Here we only point out that this map applies a square of side $2w$, centered in the origin to a set that is the drag of a simple curve along the direction determined by $\vec{v}_m$. The map $\beta_{i,j,m}^k$ maps the segment $\overline{(0,w)(0,-w)}$ to this

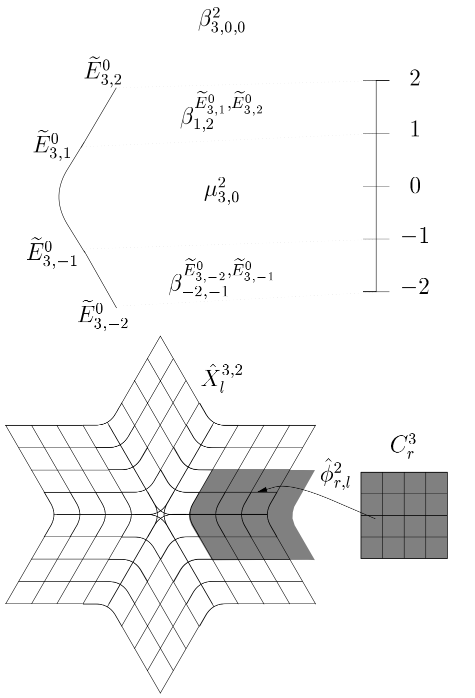

Figure 7. Transition function between regular and irregular charts.

curve. So, although the notation of $\hat{\phi}^k_{r,l}$ is few tedious, the map is very simple, and in most of his domain it is linear. The figure-7 gives a graphical idea of this construction.

Following the notation of the definition 1, if $C^n_s \subset \tilde{X}^{2nk}_l$ is another chart, then the sets $U_{\_,\_}$ are defined as

$$U_{s,r} = \hat{\phi}^k_{r,l}(C^n_r) \cap C^n_s$$

and

$$U_{r,s} = \left(\hat{\phi}^k_{r,l}\right)^{-1}(U_{s,r}).$$

Finally the transition function $\phi^k_{r,s} : U_{r,s} \to U_{s,r}$ is defined as the restriction to the set $U_{r,s}$ of the map $\hat{\phi}^k_{r,l}$, that is

$$\phi^k_{r,s} = \hat{\phi}^k_{r,l|U_{r,s}}.$$

Moreover we define $\phi^k_{s,r} = \left(\phi^k_{r,s}\right)^{-1}$ and $\phi^k_{r,r} = id$.

In appendix 11.3 is proved that these functions are well defined.

4.4 Defining the manifold

At this point we have defined all the elements necessary to construct the manifold, following definition 1.

We have a collection of connected open sets in $\mathbb{R}^2$, the charts C_i^n, that determine the proto-atlas A.

We have also defined the open sets $U_{i,j} \subset C_i^n$ for each pair of charts C_i^n, C_j^n. Notice that $U_{i,i} = C_i^n$ because $\hat{\phi}_{i,i}^k(C_i^n)$ is the identity map in C_i^n.

The transition functions $\phi_{i,j}^k : U_{i,j} \to U_{j,i}$ satisfy all the properties required in definition 1. The less trivial is the condition 3(c), the cocycle property, that is proved in theorem 2, using the results of appendix 11.3.

Thus, in this situation we can define in the proto-manifold K the equivalence relation

$$\forall x \in C_i^n, \forall y \in C_j^n, \;\; x \sim y \text{ iff } \phi_{i,j}^k(x) = y.$$

and hence the manifold M as $M = K/\sim$.

Theorem 2 *M is a k-differentiable manifold homeomorphic to the manifold defined by the control mesh.*

PROOF. The charts $C_i^n \in A$ are connected open sets in $\mathbb{R}^2$. The collection of subsets $U_{i,j} \subset C_i^n$, with $U_{i,i} = C_i^n$, has been defined for each C_i^n and C_j^n charts of A.

In corollary 9 (see appendix 11.3) we prove that the transition functions $\phi_{i,j}^k : U_{i,j} \to U_{j,i}$ are bijective and C^k differentiable maps. Moreover, by definition of transition functions the following properties hold:

(1) $\left(\phi_{i,j}^k\right)^{-1} = \phi_{j,i}^k$,
(2) $\phi_{i,i}^k(x) = x \;\; \forall x \in C_i^n$.

Thus, only the cocycle property rest to be proved, that is

$$\phi_{a,c}^k(x) = \phi_{b,c}^k \circ \phi_{a,b}^k(x) \;\; \forall x \in U_{a,b} \cap U_{a,c},$$

where C_a^n,C_b^n and C_c^n are three different charts.

If the three charts are irregular charts then the transition functions are the identity map, so there is nothing to prove. Otherwise, at minimum one of the charts must be regular.

Now, we use corollary 9 to study these cases. In corollary 9, see appendix 11.3, we prove that $\phi_{r,s}^k$ is bijective and applies faces of C_r^n to faces of C_s^n, and that corresponding points have the same parameter values. Thus, if C_r^n and C_s^n are two charts and $q \in U_{r,s} \subset C_r^n$, then $q \in C \subset C_r^n$ where C is a face of C_r^n and $q = C(\lambda, \gamma)$ with $\lambda, \gamma \in [0,1]$ are the parameters corresponding to q. Thus, using corollary 9, $q' = \phi^k_{r,s}(q) = C'(\lambda, \gamma)$, where $C' \subset C^n_s$ is the face of C^n_s that corresponds to C. Notice that this result is valid in any case:

- When C^n_r is regular and C^n_s is irregular (by corollary 9).
- When C^n_r is irregular and C^n_s is regular, using the bijectively of $\phi^k_{s,r}$ and $\phi^k_{r,s} = \left(\phi^k_{s,r}\right)^{-1}$.
- When C^n_r and C^n_s are regular charts, because in this case, transition functions are rotations and translations that apply faces to faces by mapping points with the same parameter values.

Thus, in any case, we have that if $x \in U_{a,b} \cap U_{a,c}$ then $x \in C \subset C^n_a$ and $x = C(\lambda, \gamma)$, then

$$\phi^k_{a,b}(x) = C'(\lambda, \gamma) \text{ and } \phi^k_{a,c}(x) = C''(\lambda, \gamma),$$

where C' and C'' are the representation of C in C^n_b and C^n_c respectively. And, by the same reasoning

$$\phi^k_{b,c}(C'(\lambda, \gamma)) = C''(\lambda, \gamma),$$

proving the cocycle property. Thus, M is a k-differentiable manifold.

Moreover M is homeomorphic to the manifold determined by the control mesh G. Following the construction process of M, one chart C^n_i is defined for every regular subgraph M^n_i of G,and an homeomorphism can be defined between them. In case of irregular subgraphs M^n_i of G, the corresponding chart is defined as the union of one or more charts that are included in X^n_j. Moreover, the transition functions between different charts give the overlapping between faces of the charts corresponding to the same face of the graph. Thus, both manifolds are homeomorphic. □

5 The basis functions

In this section we will define C^k-functions, with support in the defined charts, where k is one of the input parameters of the algorithm.

All the charts defined on the manifold M are rectangular, or the drag of a simple C^k curve along a straigthline, so it is useful in this situation to define tensorial product basis functions.

For the regular charts, that are squares, we define C^k-continuous B-spline tensorial product basis functions, with uniform knots distribution, and degree $k+1$.

For the irregular charts, the process is to map the irregular chart (using a C^k continuous mapping) to the square of side $2w$ centered in the origin of $\mathbb{R}^2$, where we can define a C^k-continuous B-spline tensorial product basis function.

Formally, the process is as follows: Lets $C_i^n \in \tilde{X}_l^{2nk}$ be an irregular chart, associated to the element $\tilde{e}_{a,b}^m$. Then we define $\psi_i^k : C_i^n \to \mathbb{R} \quad , \psi_i^k(x,y) = N^k\left(\phi_{a,b,m}^k(x,y)\right)$, where

$$\phi_{a,b,m}^k = \left(\hat{\phi}_{\_,l}^k\right)^{-1}, \quad \text{with} \quad \hat{\phi}_{\_,l}^k(x',y') = \beta_{a,b,m}^k(y') + (x' + \xi(n,a))\,\vec{v}_m,$$

is the map used in the previous section and N^k is a C^k-continuous tensorial product B-spline basis function of degree $k+1$, with support in $(-w,w) \times (-w,w) \subset \mathbb{R}^2$ and uniform knots distribution.

That is, we use the inverse of the transition functions to map a chart to the square $(-w,w)\times(-w,w)$ (see figure 7), and then apply a traditional tensorial product basis function. See appendix 11.3 for notation.

Notice that this functions satisfy the basic properties of a collection of basis functions, that is

- ψ_i^k is defined on the manifold M and its support is equal to the image of the chart C_i^n in M.
- ψ_i^k is C^k continuous.
- ψ_i^k is non-negative.
- An important property that is not directly satisfied by the functions ψ_i^k is to determine a partition of the unity, that is, $\sum_{C_i^n \in A} \psi_i^k(u) \neq 1$, in a general case. So, to get this property, we normalize these functions and define the basis functions Ψ_i^k as

$$\Psi_i^k(u) = \frac{\psi_i^k(u)}{\sum_j \psi_j^k(u)} \qquad \forall u \in M,$$

  which hold the desired properties.

6 The control points

To define the geometry of the resulting surface, a control point is associated to each chart. In the definition of the irregular charts, an element $\tilde{e}_{i,j}^m$ has been attached to each chart C_a^n, that has a representation in the original control mesh, let us call this element e_a. For regular charts we have not explicitly associated one element to each chart, but every regular chart C_b^n is associated to a regular subgraph M_b^n, and every subgraph M_b^n is centered on a central element, a vertex or a face, that we will also call e_b.

The element e_i corresponding to the chart C_i^n is a vertex when n is an odd number and it is a face when n is an even number. Thus, we define the control point P_i attached to the chart $C_i^n \in M$ as follows:

$$P_i = \begin{cases} v_i \text{ if } n \text{ is an odd number, and } e_i = v_i, \\ b_i \text{ if } n \text{ is even and } b_i \text{ is the baricenter of } e_i = f_i \end{cases}$$

Notice that when n is an odd number there exist a chart for every vertex of the control mesh, in this case, the control points are the vertices of the pre-processed mesh. However, if n is even, we have built a chart for every face of the original control mesh. In this case there exist a control point corresponding to each face of the control mesh. In our implementation, the baricenter of each face is chosen as control point, but there exists many other possible definitions, with the restriction that the defined control point has to be on the convex hull of the vertices of the face.

7 The surface

At this point, we are ready to define the surface. In previous sections, we have defined a manifold M from a proto-atlas A. For every chart $C_i^n \in A$, a basis function Ψ_i^k, and a control point P_i, have been built. Thus, a control point can be associated to every basis function. The basis functions are defined on the manifold M and form a partition of the unity. Thus, they can be used to obtain baricentric combinations of the control points.

Finally, the surface is defined on the manifold M, using the basis functions and the control points as follows:

$$S(u) = \sum_{C_i^n \in A} P_i \Psi_i^k(u) \quad \forall u \in M$$

The C^k continuity of the basis functions Ψ_i^k, guarantees the C^k continuity of the resulting surface S. Moreover the resulting surface is obtained from baricentric combinations of the control points. Thus, the surface is in the convex hull of the control points, which are, at same time, on the convex hull of the original mesh. Thus, we can conclude that the proposed construction method holds the convex hull property (local and global). The size of the charts (the support of the basis functions) depends on the value of n. The subgraphs M_i^n increase with the value of n, therefore the influence of each control point P_i also depends on n; in fact, it increases with the value of n.

Next we summarize the basic properties of the presented method:

(1) There is no restriction for the original mesh, although the method works with rectangular face meshes obtained from Catmull-Clark subdivisions of the original one.
(2) Where the mesh is regular, the generated surface with $n = k+1$ is equivalent to a tensorial product B-spline surface with uniform knot distribution (see [CP 99]).
(3) The points of the surface are the result of convex combinations of subsets of the control points, thus the surface has local control.
(4) The surface is included in the convex hull of the control points.
(5) The surface shape is controlled by the parameter n, that allows to obtain smoother surfaces, where every point depends on a greater number of control points, or surfaces where the normal direction changes quickly, and more closed to the control mesh, where every point depends on few control points.
(6) The computation of the manifold M is the most expensive step of the method proposed here. Nevertheless, we observe that a modification of the geometric position of any point of the original mesh does not require to recompute the manifold M, which only depends on the topology of the mesh. Only some control points have to be recomputed.

Technical properties are detailed in appendix 11.

8 Implementation and results

There are some properties of the proposed method that simplify the implementation process.

The parameter space of the surface is the manifold M, which is homeomorphic to the manifold described by the control mesh. Thus, to build the surface it is enough to go over the faces of the control mesh, once the preprocess has been aplied. The regular parts of the surface, that means, points that only belong to regular charts, are easy to define. Otherwise, the symmetry of the k-continuous regular star configuration and the symmetry of the corresponding charts is used to simplify the construction. In fact, it is only necessary go over a part of the star, correspondig to a $1/(2g)$ of the total star, when the surface is generated, as is show in figure 8. That is $2g$ points of the surface are computed simultaneously.

The construction algorithm proposed in the paper can be summarized as follows. Let $p = C(\lambda, \gamma)$ be a parameter point, then the corresponding surface point $S(p)$ is computed as

$S := 0; \quad D := 0$

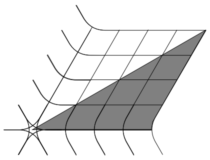

Figure 8. The grey zone represents the parameter space.

```
for all chart C_i that p ∈ C_i
   b := ψ_i^k(p)
   S := S + P_i b;  D := D + b
endfor
S(p) := S/D.
```

Now, the implementation of two different parts of the algorithm is detailled: first, the computation of the $\psi_i^k(p)$ function and second the problem to determine which irregular charts contain the point p. Both implementations are based on theorem 8.

Notice that a *regular* graph G_i can be represented in each chart C_i. For regular charts, the graph G_i coincides with the representation of the subgraph M_i^n in C_i (see section 4.2). For irregular charts, the regular graph is defined using the drag that defines the chart, that means, the graph defined by the drag of the vertices

$$\tilde{E}^m_{i+w+\xi(n,i),s}, \quad j-w-\xi(n,j) \leq s \leq j+w-\xi(n,j), \text{ and}$$

$$\tilde{E}^m_{i-1+w+\xi(n,i),s}, \quad j-w-\xi(n,j) \leq s \leq j+w-\xi(n,j)$$

(see section 4.2). Thus, only a part of G_i coincides with the representation of the control mesh in C_i.

The proof of theorem 8 shows that $\phi^k_{r,\_}$ maps a regular chart C^n_r into the C_i irregular chart, applying faces of C^n_r to faces defined by the regular graph G_i. Moreover, the corresponding points by this function have the same (λ, γ) parameters.

Using this result, the computation of the basis function value for an irregular chart C_i is as follows. If $p \in C_i$ then p is on a face C determined on G_i, so p can be represented as $p = C(\lambda, \gamma)$ (using corollari 9 notation). To compute the basis function value for p, $\psi_i^k(p)$, we maps using a transition function the chart C_i to $Q = (-w, w) \times (w, w)$, but by corollari 9 we know that $(\phi^k_{\_,\_}(C(\lambda, \gamma))^{-1} = C'(\lambda, \gamma)$, where C' is the representation of C in Q, so $\psi_i^k(p) = N(C'(\lambda, \gamma))$, where N is a tensorial product B-spline basis function.

The second problem to detail is the following: given a parametric point p we have to determine the charts that contain p. This is not straightforward in case of irregular charts. Let p be a point such that it belongs to a face C of

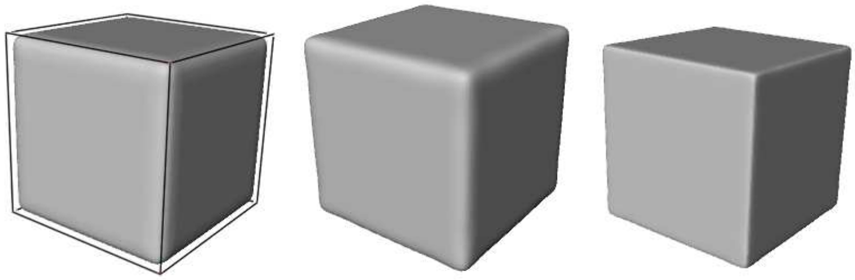

Figure 9. (a) $n = 5$, $k = 1$. (b) $n = 3$, $k = 2$. (c) $n = 3$, $k = 5$.

the k-continuous regular star cofiguration, that is, $p = C(\lambda, \gamma)$. Then, two different cases are distinguished to determine if a chart C_i contains p.

(1) If the face C is also a face of the regular graph G_i defined in a chart C_i, then p belongs to C_i.
(2) For an irregular chart C_i, if C is not a face of the graph G_i, then p may belong to C_i or not.
 Every irregular chart is associated to one element $\tilde{e}^m_{i,j}$, $i = 0, \ldots, \lfloor w \rfloor$, $|j| = \rho(n), \ldots, i + \rho(n)$. Thus, the vertex $\widetilde{E}^m_{s,0}$, $s = i + w + \xi(n, i)$, belongs to its boundary. Then, a vertex $q = E^m_{s,0}$ and three directions $\vec{v}_m$ and $\vec{v}_{m\pm1}$ can be attached to any irregular chart.
 Using these notations p can be represented as $p = q - x_p\vec{v}_m + y_p\vec{v}_{m+1}$, where $x_p, y_p \in R$ (the case $p = q - x_p\vec{v}_m + y_p\vec{v}_{m-1}$ is equivalent).
 Now, the faces of the regular graph G_i can be labeled as follows: the face that contains the point $\widetilde{E}^m_{s,0}$ as they right-down corner it is labeled as $C_{0,0}$, the rest of the faces are labeled as $C_{i,j}$ following de directions $-\vec{v}_m$ and $\vec{v}_{m\pm1}$. Using this notation, the point p belongs to the face $C_{\lfloor x'_p \rfloor, \lfloor y_p \rfloor}$, where , $x'_p = \|p - \beta^k_{s,0,m}(y_p)\|$, moreover $p = C_{\lfloor x'_p \rfloor, \lfloor y_p \rfloor}(x'_p - \lfloor x'_p \rfloor, y_p - \lfloor y_p \rfloor)$. Thus, p belongs to C_i iff $\lfloor x'_p \rfloor \leq n$ and $\lfloor y_p \rfloor \leq j + w - \xi(n, j) - 1$.

Next we comment some examples, showing the capabilities of the proposed method. We also comment the influence of the input parameters n and k to the resulting surface. All the images presented in this section have been generated using Inventor, in a Silicon Graphics.

Images in figure 9 show the influence of parameter n. Image in figure 9(a) is GC^1 while image in figure 9(c) is GC^5, although the first seems smoother than the second. This is caused by the parameter n, in case (a) $n = 5$ that is, the charts are bigger and the surface points depend on a greater number of control points than in case (c), where $n = 3$.

Images in figure 10 are generated from the same mesh (a), but the Catmull-Clark subdivision algorithm has been applied differently.

In figure 11 the curvature plots corresponding to the surface arround two vertexs of mensh (a) in figure 10 are show. Plots (a) and (b) correponds to

Figure 10. (a) Original mesh. (b) $n = 2$, $k = 1$. (c) $n = 5$, $k = 4$.

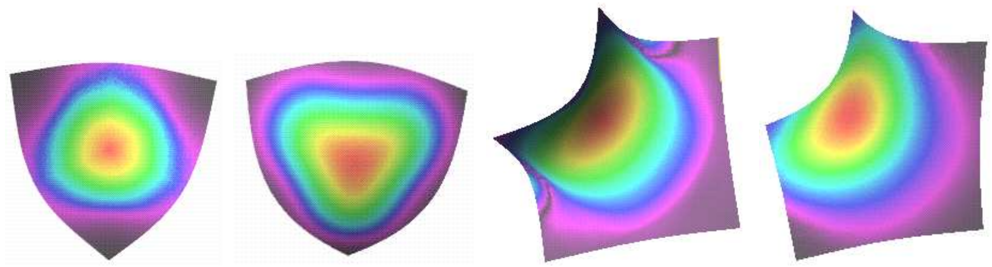

(a)$(3, 2, 3)$ (b) $(3, 4, 5)$ (c) $(5, 2, 3)$ (d) $(5, 4, 5)$

Figure 11. Curvature plots with (g, k, n).

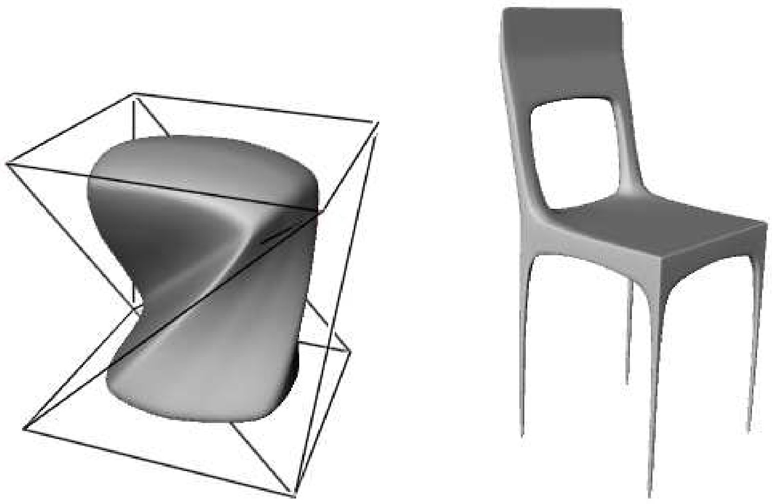

Figure 12. (a) $n = 2$, $k = 1$. (b) $n = 2$, $k = 1$.

an irregular vertex of degree 3, and continuity 2 and 4 respectivelly. Plots (c) and (d) correpond to an irregular vertex of degree 5, and continuity 2 and 4 respectivelly.

The remaining images show other possibilities of the presented method.

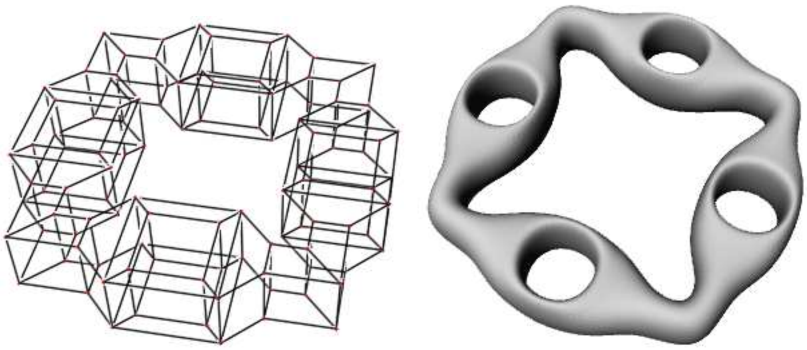

Figure 13. (a) Original mesh. (b) $n = 2$, $k = 1$.

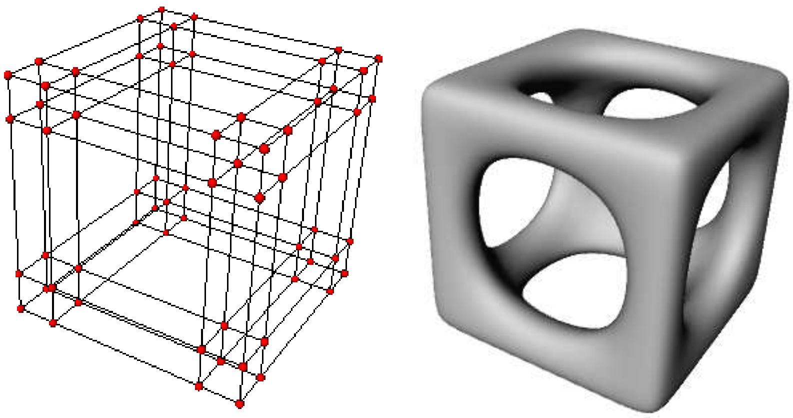

Figure 14. (a) Original mesh. (b) $n = 2$, $k = 1$.

9 Conclusions

We have presented an algorithm to construct surfaces from irregular control meshes. The method generalizes B-splines to irregular meshes. Manifold technology is used to construct this generalization. The algorithm can be summarized as follows. From an irregular mesh, a manifold M is defined. A control point is attached to each chart of M. Continuous basis functions are built with support on each chart and, finally, the analytic expression of the surface is obtained. The resulting surface is C^k-continuous, where k is an input parameter and it is included in the convex hull of the original mesh.

The algorithm has been implemented and anesthetically pleasing surfaces are obtained efficiently and easily.

10 Acknowledgments

This work has been partially supported by the CICYT, under grants TIC-98-0586-C03-01 and TIC-99-1230-C02-02.

11 Appendix

This appendix contains the technical results used in previous sections.

11.1 Regular stars

A regular star $X_l^{2n} \in \mathbb{R}^2$ is defined for any irregular vertex v_l of the mesh. Let g be the degree of the irregular vertex v_l and $\alpha = 2\pi/g$. The vertices of the regular star are defined as follows:

$$E_{0,0}^m = (0,0),$$

$$E_{i,0}^m = (i\cos(\alpha m), i\sin(\alpha m)),$$

$$E_{i,j}^m = E_{i,0}^m + E_{|j|,0}^{m+\sigma(j)},$$

for $i = 1, \ldots, 2n+1$, $|j| = 1, \ldots, 2n+1$, $m = 0, \ldots, g-1$. The operations over m are modulo g.

Then the regular star X_l^{2n} is a graph with $V = \{E_{i,j}^m\}$ as the set of vertices and $\{E_{i,j}^m, E_{i+1,j}^m\}$, $\{E_{i,j}^m, E_{i,j+1}^m\}$ as the edges of the graph.

Some properties of the vertices of the graph can be easily proved. Let us define $\vec{v}_m = \overrightarrow{E_{0,0}E_{1,0}^m}$, then the following equalities are true:

$$E_{i,j}^m = i\vec{v}_m + |j|\vec{v}_{m+\sigma(j)},$$

$$E_{i,j}^m = E_{|j|,-\sigma(j)i}^{m+\sigma(j)},$$

$$E_{i+t,j}^m = E_{i,j}^m + t\vec{v}_m.$$

The k-continuous regular star configuration, $\widetilde{X}_l^{2nk}$, is defined in a similar way, but taking the points

$$\widetilde{E}_{i,j}^m = E_{i,j}^m,$$

for $i = 1, \ldots, 2n+1$, $|j| = 1, \ldots, 2n+1$ and $m = 0, \ldots, g-1$, and the curves $\mu_{i,m}^k$ that are defined as follows. Let

$$\mu_{0,m}^k : [-1, 1] \to \mathbb{R}^2,$$

be a curve, of degree $k+1$, such that joins the segments $\overline{E_{1,0}^{m-1} E_{2,0}^{m-1}}$ and $\overline{E_{1,0}^{m+1} E_{2,0}^{m+1}}$ with GC^k continuity, and $\mu_{0,m}^k(t) = t\vec{v}_{m+\sigma(t)} + \gamma(t)\vec{v}_m$. In general $\mu_{i,m}^k$, for $i = 1, \ldots, 2n+1$ we define

$$\mu_{i,m}^k = i\vec{v}_m + \mu_{0,m}^k.$$

Finally, the new vertices of the k-continuous regular star configuration are defined as

$$\widetilde{E}_{i,0}^m = \mu_{i,m}^k(0), \tag{4}$$

for $i = 0, \ldots, 2n+1$ and $m = 0, \ldots, g-1$.

The main properties of the k-continuous regular star configuration $\tilde{X}_l^{2nk}$ are that k-continuous curves $\mu_{i,m}^k$ join the vertices $\tilde{E}_{i,1}^m$ and $\tilde{E}_{i,-1}^m$ and that the irregular vertex E_{00} blows up into $g = degree(v_l)$ different vertices $\tilde{E}_{00}^j$, where $j = 0, \ldots, g-1$.

Figure 4 is a graphical representation of a k-continuous regular star with $g = 6$.

11.2 Manifolds with boundary

Let $G = (V, E)$ be the mesh obtained once the pre-process explained in section 4.1 has been applied to the original mesh. To ensure that the proposed method is valid to deal with meshes with boundary the graph G is surrounded by $\lceil \frac{n}{2} \rceil + 1$ layers of regular mesh in order to simplify the construction of the charts along the boundaries. Let us call $G' = (V', E')$ the extended graph.

Then the process used to construct the charts, presented in section 4.2, is applied to G' as follows. A subgraph $M_i^n \subset G'$ is built for every vertex or face of $G \subset G'$, depending on whether n is odd or even respectively. Notice that no subgraph is built for the elements that only belong to G' (see figure 15).

The $\lceil \frac{n}{2} \rceil + 1$ layers of regular mesh that surround G ensure that the subgraphs $M_i^n \subset G'$ can be classified as regular, subgraphs with all the vertices regular,

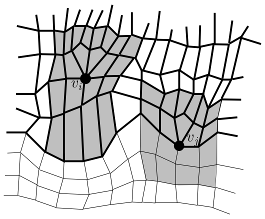

Figure 15. Mesh with boundary. Subgraphs M_i^3 and M_j^3 are shown.

or irregular, subgraphs with one irregular vertex. Thus the remaining of the process presented in the previous sections can be applied exactly, using as parameter space the manifold obtained from the charts associated to subgraphs $M_i^n \subset G \subset G'$.

Moreover, the geometry of the vertices added to the control mesh G is never used, because the new vertices are not associated to any chart and no control point is attached to them, thus it is not necessary to define their geometry.

11.3 Transition functions

In this section we present technical results useful to understand the behavior of the transition functions and we also prove that they are well defined.

However, first of all some properties of the linear interpolation are presented. Their proof is straightforward.

Let us define
$$X_{a,b} : [0,1] \to \overline{ab}$$
where $\overline{ab} \in \mathbb{R}$ or $\mathbb{R}^2$ as
$$X_{a,b}(t) = (1-t)a + tb,$$
and the map
$$\beta_{a,b}^{A,B} : \overline{ab} \to \overline{AB}$$
where $\overline{AB} \in \mathbb{R}^2$ and
$$\beta_{a,b}^{A,B}(X_{a,b}(t)) = X_{A,B}(t), \quad \forall t \in [0,1].$$

Lemma 3 *Lets $\overline{ab} \in \mathbb{R}^2$, $a \neq b$, a segment. The linear interpolation*
$$X_{a,b} : [0,1] \to \overline{ab},$$
where $X_{a,b}(t) = (1-t)a + tb$, satisfy:

(1) Is bijective and C^∞.

(2) Lets $\overline{a'b'} \in \mathbb{R}^2$, then

$$\frac{1}{2}\left(X_{a,b}(t) + X_{a',b'}(t)\right) = X_{\frac{a+a'}{2},\frac{b+b'}{2}}(t), \quad \forall t \in [0,1].$$

(3) Lets $p_{|i}$, the i-th p coordinate, then

$$X_{a,b}(t)_{|i} = X_{a_{|i},b_{|i}}(t), \quad \forall t \in [0,1].$$

(4) Lets $\overline{ef} \subseteq [0,1]$, $e \neq f$, then

$$X_{a,b}(X_{e,f}(t)) = X_{X_{a,b}(e),X_{a,b}(f)}(t), \quad \forall t \in [0,1].$$

Lemma 4 *Lets $\overline{ab} \in \mathbb{R}^2$, $a \neq b$ and $\overline{AB} \in \mathbb{R}^2$, $A \neq B$. We define*

$$\beta_{a,b}^{A,B} : \overline{ab} \to \overline{AB},$$

as

$$\beta_{a,b}^{A,B}\left(X_{a,b}(t)\right) = X_{A,B}(t), \quad \forall t \in [0,1].$$

Then $\beta_{a,b}^{A,B}$ is bijective and C^∞. If $\overline{ef} \subset \overline{ab}$, then

$$\beta_{a,b}^{A,B} \circ X_{e,f} = X_{\beta_{a,b}^{A,B}(e),\beta_{a,b}^{A,B}(f)}.$$

Now, let us use these properties to study the embedding of a regular chart to the k-continuous regular star. Let C_r^n be a regular chart such that all its vertices can be identified in the k-continuous regular star $\tilde{X}_l^{2nk}$. Then, there exists $\tilde{e}_{i,j}^m \in \tilde{X}_l^{2nk}$ an element which can be associated to C_r^n.

Then, the embedding of C_r^n in $\tilde{X}_l^{2nk}$ is defined as:

$$\hat{\phi}_{r,l}^k : C_r^n \to \mathbb{R}^2$$

$$\hat{\phi}_{r,l}^k(x,y) = \beta_{i,j,m}^k(y) + (x + \xi(n,i))\,\vec{v}_m, \tag{5}$$

where $\beta_{i,j,m}^k : (-w,w) \to \mathbb{R}^2$ is:

When $|j| \leq \lceil w \rceil$:

$$\beta^k_{i,j,m}(y) = \begin{cases} \beta^{\tilde{E}^m_{i,1}, \tilde{E}^m_{i,j+w-\xi(n,j)}}_{\xi(n,j)+1-j,w}(y), & \text{if } w > y \geq \xi(n,j)+1-j, \\ \mu^k_{im}\left(y+j-\xi(n,j)\right), & \text{if } \xi(n,j)-1-j < y < \\ & < \xi(n,j)+1-j, \\ \beta^{\tilde{E}^m_{i,j-w-\xi(n,j)}, \tilde{E}^m_{i,-1}}_{-w,\xi(n,j)-1-j}(y), & \text{if } -w < y \leq \xi(n,j)-1-j. \end{cases}$$

When $|j| > \lceil w \rceil$:

$$\beta^k_{i,j,m}(y) = \beta^{\tilde{E}^m_{i,j-w-\xi(n,j)}, \tilde{E}^m_{i,j+w-\xi(n,j)}}_{-w,w}(y), \qquad -w < y < w.$$

See figure 7 for a graphical example.

Next lemma proves that the map $\beta^k_{i,j,m}$, maps representations of vertices from regulars charts to the corresponding representation in a k-continuous regular star.

Lemma 5 *The map $\beta^k_{i,j,m}$ is bijective and GC^k. Moreover, it satisfies*

$$\beta^k_{i,j,m}(t) = \tilde{E}^m_{i,j+t-\xi(n,j)}, \quad \textit{for} \quad t = -w+r, \quad \textit{where} \quad r = 0, \ldots, n+1.$$

PROOF.

Case $|j| > \lceil w \rceil$: $\beta^k_{i,j,m}$ is a linear interpolation. In particular, it has been defined as:

$$\beta^k_{i,j,m} = \beta^{\tilde{E}^m_{i,j-w-\xi(n,j)}, \tilde{E}^m_{i,j+w-\xi(n,j)}}_{-w,w}.$$

Notice that the condition $|j| > \lceil w \rceil$ imply that $\tilde{E}^m_{i,j-w-\xi(n,j)}\tilde{E}^m_{i,j+w-\xi(n,j)}$ determines a straight segment in the regular star which is composed by edges of the k-continuous regular star. Thus, by lemma 4, it is bijective and C^∞.

The points

$$\tilde{E}^m_{i,j+t-\xi(n,j)} \text{ for } t = -w+r, r = 0, \ldots, n+1,$$

are uniformly distributed in the segment $\overline{\tilde{E}^m_{i,j-w-\xi(n,j)}\tilde{E}^m_{i,j+w-\xi(n,j)}}$, thus,

$$\tilde{E}^m_{i,j+t-\xi(n,j)} = X_{\tilde{E}^m_{i,j-w-\xi(n,j)}, \tilde{E}^m_{i,j+w-\xi(n,j)}}\left(\frac{t+w}{2w}\right).$$

Moreover $t = X_{-w,w}(\frac{t+w}{2w})$, thus,

$$\beta^k_{i,j,m}(t) = \beta_{-w,w}^{\tilde{E}^m_{i,j-w-\xi(n,j)},\tilde{E}^m_{i,j+w-\xi(n,j)}} \circ X_{-w,w}(\frac{t+w}{2w}) =$$

$$= X_{\tilde{E}^m_{i,j-w-\xi(n,j)},\tilde{E}^m_{i,j+w-\xi(n,j)}}\left(\frac{t+w}{2w}\right) = \tilde{E}^m_{i,j+t-\xi(n,j)}.$$

Case $|j| \leq \lceil w \rceil$: In this case the segment $[-w, w]$ is applied over the continuous regular star, using a k-continuous map with three different parts.

- The segment $[\xi(n,j)+1-j, w]$ is applied by linear interpolation over the segment $\overline{\tilde{E}^m_{i,1}\tilde{E}^m_{i,j+w-\xi(n,j)}}$, that is, in this interval

  $$\beta^k_{i,j,m} = \beta_{\xi(n,j)+1-j,w}^{\tilde{E}^m_{i,1},\tilde{E}^m_{i,j+w-\xi(n,j)}},$$

  then, using the previous reasoning

  $$\tilde{E}^m_{i,j+t-\xi(n,j)} = X_{\tilde{E}^m_{i,1},\tilde{E}^m_{i,j+w-\xi(n,j)}}\left(\frac{t+j-1-\xi(n,j)}{w+j-1-\xi(n,j)}\right)$$

  and

  $$t = X_{\xi(n,j)+1-j,w}(\frac{t+j-1-\xi(n,j)}{w+j-1-\xi(n,j)}),$$

  so

  $$\beta^k_{i,j,n}(t) = \tilde{E}^m_{i,j+t-\xi(n,j)}.$$

- The segment $[-w, xi(n,j)-1-j]$ is applied over $\overline{\tilde{E}^m_{i,j-w-\xi(n,j)}\tilde{E}^m_{i,-1}}$ by linear interpolation, and the previous reasoning is valid in this case.
- Finally, the segment $[\xi(n,j)-1-j, \xi(n,j)+1-j]$ is applied over the regular star using the $\mu^n_{i,m}$ map. In fact we define

  $$\beta^k_{i,j,m}(t) = \mu^n_{i,m}(t+j-\xi(n,j)),$$

  when $\xi(n,j)-1-j < t < \xi(n,j)+1-j$. Notice that this interval has length two and it is centered in $\xi(n,j)-j$. Moreover, the previous definition makes sense because when $\xi(n,j)-1-j < t < \xi(n,j)+1-j$, then $t+j-\xi(n,j)$ describes the interval $(-1,1)$, and

  $$\beta^k_{i,j,m}(\xi(n,j)-j) = \mu^k_{i,m}(0) = \tilde{E}^m_{i,0}.$$

The three parts of the $\beta^k_{i,j,m}$ function are bijective, and their images have no common points, thus $\beta^k_{i,j,m}$ is bijective. Moreover, each one of these parts of the function is C^∞, because two of them are linear interpolations and the other is polynomial. The map $\mu^k_{i,m}$ glue with GC^k continuity the segments $\overline{\tilde{E}^m_{i,-1}\tilde{E}^m_{i,-2}}$ and $\overline{\tilde{E}^m_{i,1}\tilde{E}^m_{i,2}}$, joining the points $\tilde{E}^m_{i,-1}$, $\tilde{E}^m_{i,1}$. These two points are the endpoints of the images of the linear interpolation parts of $\beta^k_{i,j,m}$. Then we can conclude that $\beta^k_{i,j,m}$ has GC^k continuity. $\square$

Lemma 6 $\forall \lambda \in \mathbb{R}$, *and* $u, v \in (-w, w), u \neq v$,

$$\beta^k_{i,j,m}(u) - \beta^k_{i,j,m}(v) \neq \lambda \vec{v}_m,$$

where $\vec{v}_m = \overrightarrow{\tilde{E}^m_{20}\tilde{E}^m_{10}}$.

PROOF. The proof of this lemma follows the definition of the k-continuous regular star and the image of the $\beta^k_{i,j,m}$ function, which has been studied in the proof of lemma 5. $\square$

Next lemma proves that the maps $\hat{\phi}^k_{r,l}$ map representations of vertices to representations of vertices.

Lemma 7 *The maps* $\hat{\phi}^k_{r,l} : C^n_r \to \mathbb{R}^2$ *satisfy:*

(1) $\hat{\phi}^k_{r,l}(t_1, t_2) = \tilde{E}^m_{i+t_1+\frac{1}{2}\rho(n), j+t_2-\xi(n,j)}, \quad \forall (t_1, t_2) = (-w + r, -w + s),$ *where* $r, s = 0, \ldots, n + 1$.

(2) If $X_{e,f}(t) \notin (\xi(n, j) - 1 - j, \xi(n, j) + 1 - j)$ *then*

$$\hat{\phi}^k_{r,l}(X_{e,f}(t)) = X_{\hat{\phi}^k_{r,l}(e), \hat{\phi}^k_{r,l}(f)}(t).$$

PROOF. By lemma 5

$$\hat{\phi}^k_{r,l}(t_1, t_2) = \beta^k_{i,j,m}(t_2) + (t_1 + \frac{1}{2}\rho(n))\vec{v}_m = \tilde{E}^m_{i,j+t_2-\xi(n,j)} + (t_1 + \frac{1}{2}\rho(n))\vec{v}_m.$$

But we know that $\tilde{E}^m_{i,j} + t\vec{v}_m = \tilde{E}^m_{i+t,j}$, for $t \in \mathbb{Z}$. Moreover, $w + \frac{1}{2}\rho(n) \in \mathbb{Z}$, then $t_1 + \frac{1}{2}\rho(n) \in \mathbb{Z}$, so

$$\hat{\phi}^k_{r,l}(t_1, t_2) = \tilde{E}^m_{i+t_1+\frac{1}{2}\rho(n), j+t_2-\xi(n,j)}.$$

If $X_{e,f}(t) \notin (\xi(n, j) - 1 - j, \xi(n, j) + 1 - j)$, then $\beta^k_{i,j,m}$ is as $\beta^{A,B}_{a,b}$ (lemma 4). Using lemma 3 and lemma 4 we have

$$\begin{aligned}
\hat{\phi}^k_{r,l}(X_{e,f}(t)) &= \beta^k_{i,j,m}(X_{e_{|y}, f_{|y}}(t)) + \left(X_{e_{|x}, f_{|x}}(t) + \frac{1}{2}\rho(n)\right)\vec{v}_m = \\
&= X_{\beta^k_{i,j,m}(e_{|y}), \beta^k_{i,j,m}(f_{|y})}(t) + X_{(e_{|x}+\frac{1}{2}\rho(n))\vec{v}_m, (f_{|x}+\frac{1}{2}\rho(n))\vec{v}_m}(t) = \\
&= X_{\beta^k_{i,j,m}(e_{|y})+(e_{|x}+\frac{1}{2}\rho(n))\vec{v}_m, \beta^k_{i,j,m}(f_{|y})+(f_{|x}+\frac{1}{2}\rho(n))\vec{v}_m}(t) = \\
&= X_{\hat{\phi}^k_{r,l}(e), \hat{\phi}^k_{r,l}(f)}(t).
\end{aligned}$$

$\square$

Theorem 8 *Let C_r^n be a regular chart which can be embedded into the k-continuous regular star $\widetilde{X}_l^{2nk}$. Then the map $\hat{\phi}_{r,l}^k : C_r^n \to \mathbb{R}^2$ is injective, GC^k and maps faces of C_r^n to faces of $\widetilde{X}_l^{2nk}$.*

PROOF. $\hat{\phi}_{r,l}^k$, is the drag of $\beta_{i,j,m}^k$ in the $\vec{v}_m$ direction. So $\hat{\phi}_{r,l}^k$, by lemma 5, is GC^k.

If $p, q \in \mathbb{R}^2, p \neq q$, and

$$\beta_{i,j,m}^k(p_{|y}) + (p_{|x} + \frac{1}{2}\rho(n))\vec{v}_m = \beta_{i,j,m}^k(q_{|y}) + (q_{|x} + \frac{1}{2}\rho(n))\vec{v}_m,$$

then

$$\beta_{i,j,m}^k(p_{|y}) - \beta_{i,j,m}^k(q_{|y}) = q_{|x}\vec{v}_m - p_{|x}\vec{v}_m,$$

that contradicts lemma 6, so $\hat{\phi}_{r,l}^k$ is injective.

If P is a parallelogram, with vertices a_1, a_2, a_2, a_4 and edges $\overline{a_1a_2}$, $\overline{a_2a_3}$, $\overline{a_3a_4}$ and $\overline{a_4a_1}$, every point $p \in P$ can be represented uniquely using two real numbers $\lambda, \gamma \in [0, 1]$ as

$$p = P(\lambda, \gamma) = X_{X_{a_1,a_4}(\gamma), X_{a_2,a_3}(\gamma)}(\lambda).$$

A regular chart C_r^n is composed by the faces $C_{a,b}$ with $a, b = -w, \ldots, w-1$. The faces $C_{a,b}$ are squares, with vertices $(a+e, b+f)$ where $e, f = 0, 1$.

The regular faces of the configurations $\widetilde{X}_l^{2nk}$, $C_{a,b}^m$, for $a = 1, \ldots, 2n$, $|b| = 0, \ldots, 2n$ and $m = 0, \ldots, g-1$, are determined by the points $\tilde{E}_{a+e,b+f}^m$, where $e, f = 0, 1$, and are of two types:

- If $b \neq 0, -1$ are parallelograms with edges

$$\overline{\tilde{E}_{a,b}^m \tilde{E}_{a+1,b}^m}, \overline{\tilde{E}_{a+1,b}^m \tilde{E}_{a+1,b+1}^m}, \overline{\tilde{E}_{a+1,b+1}^m \tilde{E}_{a,b+1}^m} \quad \text{and} \quad \overline{\tilde{E}_{a,b+1}^m \tilde{E}_{a,b}^m}.$$

- If $b = 0, -1$ they are determined by the edges

$$\overline{\tilde{E}_{a,b}^m \tilde{E}_{a+1,b}^m}, \overline{\tilde{E}_{a,b+1}^m \tilde{E}_{a+1,b+1}^m}$$

  and the B-spline curves $\mu_{a,m}^k(u)$ and $\mu_{a+1,m}^k(u)$, for $u \in [b, b+1]$.

  In this case, every point p of the face $C_{a,b}^m$ can be represented uniquely by two real numbers $\lambda, \gamma \in [0, 1]$ as

$$p = C_{a,b}^m(\lambda, \gamma) = X_{\mu_{a,m}^k(X_{b,b+1}(\gamma)), \mu_{a+1,m}^k(X_{b,b+1}(\gamma)}(\lambda)$$

Now, let us prove that the function $\hat{\phi}_{r,l}^k$ applies any face $C_{a,b}$ of C_r^n to a face of $\tilde{X}_l^{2nk}$.

Let $C_{a,b}$ be a C_r^n face, and suppose that C_r^n is associated to the element $\tilde{e}_{i,j}^m \in \tilde{X}_l^{2nk}$. Using the definition of the element $\tilde{e}_{i,j}^m$ (see (2)), then

$$\hat{\phi}_{r,l}^k \left(-\frac{1}{2}\rho(n), \xi(n,j) \right) = \tilde{E}_{i,j}^m,$$

thus the vertices of the face $C_{a,b}$ are applied to the vertices of the face

$$C^m_{i+a+\frac{1}{2}\rho(n), j+b-\xi(n,j)} \subset \tilde{X}_l^{2nk},$$

using lemma 7.

Now we are ready to show that the face $C_{a,b}$ is applied to $C^m_{i+a+\frac{1}{2}\rho(n), j+b-\xi(n,j)}$.

The remaining of the proof follows a simple idea, although the notation makes it a little tedious. We use the fact that $\hat{\phi}_{r,l}^k$ is the drag of $\beta_{i,j,m}^k$, which is, in most of the cases, a linear interpolation.

To simplify the notation, we write $a_{in} = i + a + \frac{1}{2}\rho(n)$ and $b_{jn} = j + b - \xi(n,j)$. Let $p = C_{a,b}(\lambda, \gamma) = X_{X_{(a,b),(a,b+1)}(\gamma), X_{(a+1,b),(a+1,b+1)}(\gamma)}(\lambda)$ be a point in $C_{a,b}$.

If $b_{jn} \neq 0, -1$, then $\hat{\phi}_{r,l}^k$ is a linear interpolation between two parallelograms and by lemma 7

$$\hat{\phi}_{r,l}^k(p) = \hat{\phi}_{r,l}^k \left(X_{X_{(a,b),(a,b+1)}(\gamma), X_{(a+1,b),(a+1,b+1)}(\gamma)}(\lambda) \right) =$$

$$= X_{\hat{\phi}_{r,l}^k \left(X_{(a,b),(a,b+1)}(\gamma) \right), \hat{\phi}_{r,l}^k \left(X_{(a+1,b),(a+1,b+1)}(\gamma) \right)}(\lambda) =$$
$$= X_{X_{\hat{\phi}_{r,l}^k(a,b), \hat{\phi}_{r.l}^k(a,b+1)}(\gamma), X_{\hat{\phi}_{r,l}^k(a+1,b), \hat{\phi}_{r,l}^k(a+1,b+1)}(\gamma)}(\lambda) =$$
$$= X_{X_{\tilde{E}^m_{a_{in},b_{jn}}, \tilde{E}^m_{a_{in},b_{jn}+1}}(\gamma), X_{\tilde{E}^m_{a_{in}+1,b_{jn}}, \tilde{E}_{a_{in}+1,b_{jn}+1}(\gamma)}}(\lambda) =$$
$$= C_{a_{in},b_{jn}}(\lambda, \gamma) = C^m_{i+a+\frac{1}{2}\rho(n), j+b-\xi(n,j)}(\lambda, \gamma).$$

If $b_{jn} = 0, -1$, then $C^n_{a_{in},b_{jn}}$ has two edges which are B-spline curves. In this case $p_{|y} = X_{b,b+1}(\gamma) \in (\xi(n,j) - 1 - j, \xi(n,j) + 1 - j)$ thus

$$\beta_{ijm}^k(b + \gamma) = \mu_{i,m}^k(b + \gamma + j - \xi(n,j)).$$

and

$$\hat{\phi}_{r,l}^k(p) = \beta_{ijm}^k(b + \gamma) + (a + \lambda + \frac{1}{2}\rho(n))\vec{v}_m =$$
$$= \mu_{i,m}^k(b + \gamma + j - \xi(n,j)) + (a + \frac{1}{2}\rho(n))\vec{v}_m + \lambda\vec{v}_m.$$

Moreover $\vec{v}_m = \mu_{a_{in}+1,m}^k(u) - \mu_{a_{in},m}^k(u)$, for $u \in [-1, 1]$, thus

$$\mu_{i,m}^k(b + \gamma + j - \xi(n,j)) + (a + \frac{1}{2}\rho(n))\vec{v}_m + \lambda\vec{v}_m.$$

$$= \mu^k_{i,m}(X_{b_{jn},b_{jn}+1}(\gamma)) + \left(a + \frac{1}{2}\rho(n)\right)\vec{v}_m +$$
$$+\lambda\left(\mu^k_{a_{in}+1,m}\left(X_{b_{jn},b_{jn}+1}(\gamma)\right) - \mu^k_{a_{in},m}\left(X_{b_{jn},b_{jn}+1}(\gamma)\right)\right),$$

but,

$$\mu^k_{i,m}\left(X_{b_{jn},b_{jn}+1}(\gamma)\right) + \left(a + \frac{1}{2}\rho(n)\right)\vec{v}_m = \mu^k_{a_{in},m}\left(X_{b_{jn},b_{jn}+1}(\gamma)\right),$$

so

$$\hat{\phi}^k_{r,l}(p) = (1-\lambda)\mu^k_{a_{in},m}\left(X_{b_{jn},b_{jn}+1}(\gamma)\right) + \lambda\mu^k_{a_{in}+1,m}\left(X_{b_{jn},b_{jn}+1}(\gamma)\right) =$$
$$= X_{\mu^k_{a_{in},m}\left(X_{b_{jn},b_{jn}+1}(\gamma)\right),\mu^k_{a_{in}+1,m}\left(X_{b_{jn},b_{jn}+1}(\gamma)\right)}(\lambda) =$$
$$= C_{a_{in},b_{jn}}(\lambda,\gamma) = C^m_{i+a+\frac{1}{2}\rho(n),j+b-\xi(n,j)}(\lambda,\gamma).$$

□

Corollary 9 *The transition functions $\phi^k_{r,s}$ are bijective, GC^k and apply faces of C^n_r to faces of C^n_s. Moreover, the corresponding points by these functions have the same (λ,γ) parameters.*

References

[BG 88] M.Berger, B.Gostiaux, *Differential geometry: Manifolds, curves and surfaces*, Graduate texts in mathematics 115, Springer-Verlag, 1988.

[CC 78] E.Catmull, J.Clark, *Recursively generated B-spline surfaces on arbitrary topological meshes*, Computer Aided Design, Vol 10, No 10, pp 350-355, 1978.

[CP 99] J. Cotrina, N. Pla, *Modelling surfaces from planar irregular meshes*, Computer Aided Geometric Design17, pp 1-15, 2000.

[Do 76] M.P. do Carmo, *Differential geometry of curves and surfaces*, Prentice-Hall, Inc., 1976.

[D 78] D.Doo, *A subdivision algorithm for smoothing irregularly shaped polyhedrons*, Proceedings on interactive techniques in computer aided design, Bologna, pp 157-165, 1978.

[Far 90] G. Farin, *Curves and Surfaces for computer aided geometric design. A Practical Guide*, Second Edition, Academic Press, 1990.

[Fl 97] M.S.Floater, *Parameterization and smooth approximation of surface triangulations*, Computer Aided Geometric Design 14, pp 231-250, 1997.

[GH 95] C.M.Grimm, J.F.Hughes, *Modeling surfaces of arbitrary topology using manifolds*, SIGGRAPH'95, pp 359-368, 1995.

[GZ 94] J.A.Gregory, J.Zhou, *Filling polygonal holes with bicubic patches*, Computer Aided Geometric Design 11, pp 391-410, 1994.

[HoMo 90] K.Hölling, H.Mögerle *G-splines*, Computer Aided Geometric Design, 7, pp 197-207, 1990.

[LD 89] C.T.Loop, T.D.DeRose, *A multisided generalization of Bézier surfaces*, ACM transactions on Graphics, Vol 8, No 3, pp 204-234, 1989.

[LD 90] C.T.Loop, T.D.DeRose, *Generalized B-spline surfaces of arbitrary topology*, Computer Graphics, Vol 24, No 4, pp 347-356, 1990.

[Lo 94] C.Loop, *Smooth spline surfaces over irregular meshes*, Proceedings of SIGGRAPH'94, pp 303-310, 1994.

[Ma 71] C.W.Marshall, *Applied Graph Theory*, Wiley, New York, 1971.

[Pe 95] J. Peters, *Biquartic C^1-surface splines over irregular meshes*, Computer Aided Design, Vol 27, No 12, pp 895-903, 1995.

[Prau 97] H.Prautzsch *Freeform splines*, Computer Aided Geometric Design, 14, pp 201-206, 1997.

[Reif 95] U. Rief, *Biquadratic G-spline surfaces* Computer Aided Geometric Design 12, pp 193-205, 1995.

[Sei 91] H.P.Seidel, *Polar forms and triangular B-spline Surfaces*, Tutorial of SIGGRAPH'91, pp 8.1-8.52.

[Stam 98] J. Stam *Exact evaluation of Catmull-Clark subdivision surfaces at arbitrary parameter values*, Proceedings of SIGGRAPH'98, pp 395-204, 1998.

[SZSS 98] T.W. Sederberg, J.Zheng, D.Sewell, M.Sabin, *Non uniform recursive subdivision surfaces*, Proceedings of SIGGRAPH'98, pp 387-394, 1998.

[Wh 73] A.T.White, *Graphs, groups and surfaces*, North Holland Publishing Company, 1973.

[Wi 86] J.J. Van Wijk, *Bicubic patches for approximating non-rectangular control-point meshes*, Computer Aided Geometric Design 3, pp 1-13, 1986.